

Structural and electronic properties of Ge-Te clusters

Ramkumar Natarajan

Department of Civil and Materials Engineering, University of Illinois at Chicago, Chicago, Illinois 60607, USA

Serdar Ögüt

Department of Physics, University of Illinois at Chicago, Chicago, Illinois 60607, USA

(Received 29 January 2003; published 26 June 2003)

The atomic and electronic structures of IV-VI semiconductor clusters Ge_nTe_m ($n+m \leq 10$) are investigated using a real-space higher-order finite-difference *ab initio* pseudopotential method. Langevin molecular dynamics coupled to a simulated annealing procedure allows us to find the geometries of ground-state and low-energy structures for $n=m$ and $n=m \pm 1$. The binding energies, energy gaps, dipole moments, static polarizabilities, and vibrational frequencies are calculated. The results are compared with available experimental data and existing calculations on group IV, III-V, and II-VI semiconductor clusters. The polarizabilities of the clusters considered are found to be very close to the bulk value with a nonmonotonic variation as a function of the cluster size. Most of the lowest-energy structures have lower symmetries and larger energy gaps compared to other isomers, indicating a higher stability of distorted Ge_nTe_m clusters, reminiscent of the Peierls distortions observed in the solid and liquid phases of GeTe.

DOI: 10.1103/PhysRevB.67.235326

PACS number(s): 61.46.+w, 36.40.Cg

I. INTRODUCTION

Being an intermediate state of matter between free atoms and bulk solids, atomic clusters, with their reduced dimensionality and large surface-to-volume ratio, have unique structural and electronic properties.^{1,2} The strong size dependence of these properties potentially makes it possible to fine-tune them for particular applications. As such, studies aimed at understanding the underlying physics of atomic clusters as a function of size are both fundamentally and technologically important. Most of the studies on small semiconductor clusters have so far been focused on group IV, III-V, and II-VI clusters. Recently small clusters of the prototype IV-VI semiconductor GeTe have attracted experimental interest.^{3,4} The measured static polarizabilities were observed to be strongly temperature dependent for certain sizes. It was suggested that this strong temperature dependence might be linked to the structural instabilities observed in bulk GeTe. These observations combined with the limited information available from experimental studies provide a strong motivation for a theoretical study of Ge_nTe_m clusters.

GeTe is a rather interesting material based on the existence of structural phase transitions in *both* the crystalline and liquid states. It has long been known that bulk GeTe undergoes a structural phase transition near 700 K from a high-temperature *B1* rocksalt phase to a lower-symmetry low-temperature *A7* rhombohedral phase.⁵ This transition is due to a three-dimensional Peierls distortion,⁶ in which a lower-symmetry structure with a gap at the Fermi level is energetically favored over a metallic high-symmetry structure with a half-filled *p* band.⁷ Recently, theoretical and experimental evidence were presented for a similar Peierls distortion in the liquid phase of GeTe right above the melting temperature near 1000 K.⁸ A combination of *ab initio* molecular dynamics simulations with neutron scattering experiments showed that a high degree of alternating chemical order, reminiscent of the low-temperature *A7* crystalline phase,

appeared at the melting temperature and disappeared upon going to higher temperatures.⁹ This fascinating behavior observed in bulk and liquid GeTe certainly raises the question whether similar phenomena can be observed in Ge_nTe_m clusters.

The goal of this paper is to predict and investigate the atomic and electronic structures of small clusters in this important IV-VI semiconductor and to make comparisons with available experimental data and existing calculations for other semiconductor clusters. So far, the only existing calculation on Ge_nTe_m clusters¹⁰ includes up to four atoms and addresses the low-energy structures and the associated dipole moments. While we agree with the findings of this study in general, we find a lower energy distorted structure for GeTe_2 . In addition, we consider clusters up to ten atoms and calculate various other properties such as static polarizabilities, binding energies, and vibrational frequencies. Our calculations show that Ge_nTe_m clusters in general adopt lower-symmetry structures compared to group IV, III-V, and II-VI semiconductor clusters. The widening of the gap from the highest occupied molecular orbital (HOMO) to the lowest unoccupied molecular orbital (LUMO) upon going to lower-symmetry structures is usually accompanied by a gain in electronic energy, similar to the Peierls distortions observed in the liquid and solid phases of GeTe. This behavior is further investigated for the case of Ge_2Te_2 using vibrational frequencies. The low symmetry observed in the ground-state structures of many Ge_nTe_m clusters gives rise to rather large dipole moments, suggesting a large ionic contribution to the finite-temperature static polarizabilities. In contrast with the group IV, III-V, and II-VI clusters, where the polarizabilities approach the bulk value from above (decreasing as the cluster size increases), the polarizabilities of Ge_nTe_m clusters do not have a strong size dependence and are scattered around the bulk value. While some of the calculated polarizabilities are in good agreement with the experimental measurements, there still remain puzzling discrepancies between theoretical

values (at $T=0$ K) and the significantly small values measured at 38 K and some anomalously large values measured at 300 K.

II. COMPUTATIONAL METHODS

Our calculations were performed entirely in real space using the higher-order finite-difference *ab initio* pseudopotential method.¹¹ We used Troullier-Martins pseudopotentials¹² in nonlocal form¹³ generated from reference configurations of $4s^2 4p^2 4d^0$ (with core radii $r_{cs}=2.6$, $r_{cp}=2.5$, $r_{cd}=2.8$ a.u.) and $5s^2 5p^4 5d^0$ ($r_{cs}=2.6$, $r_{cp}=2.4$, $r_{cd}=3.2$ a.u.) for Ge and Te, respectively. For Te, scalar relativistic pseudopotentials were constructed using nonlinear core corrections.¹⁴ The calculations were performed within the local density approximation (LDA) using the Ceperley-Alder exchange-correlation functional.¹⁵ In order to check the sensitivity of the results to the form of the exchange-correlation functional, some small cluster calculations were repeated using a generalized gradient approximation (GGA) functional.¹⁶ In the real-space higher-order finite-difference method, the Kohn-Sham equations were solved on a three-dimensional Cartesian grid of uniform grid spacing $h=0.5$ a.u. Convergence tests were carried out by reducing h down to 0.25 a.u. in some cases. The clusters were placed in a spherical domain, outside which the wave functions were required to vanish. The radius of each sphere was chosen so that the outermost atom was at least 7 a.u. away from the boundary. For polarizability calculations, the radius of the sphere was increased, since the results are rather sensitive to the tails of the wave functions. In this case, the atoms were at least 12 a.u. away from the sphere boundary.

To find the ground-state atomic structures of Ge_nTe_m clusters, we used Langevin molecular dynamics (LMD) coupled to a simulated annealing procedure.¹⁷ The simulations were started from a random atomic configuration at 2800 K, and the temperature was reduced in steps of 500 K to final value of 300 K. At each temperature the clusters were equilibrated for 90–100 time steps. Each time step was chosen to be 7 fs. During LMD simulations, we used a friction coefficient 5×10^{-4} a.u. After 300 K, the clusters were quenched to zero temperature, and the ground-state atomic configurations were determined by the initially scaled variable-metric minimization scheme of Broyden, Fletcher, Goldfarb, and Shanno.¹⁸ For a binary cluster such as Ge-Te, the choice of the initial atomic configuration plays an important role in finding the energetically favorable structures. At the start of the LMD simulations, we typically placed the Ge and Te atoms at random positions around each other at distances of 1–1.3 times the dimer bond length. In spite of the randomness, sampling the full phase space in a finite amount of time may not always be possible. In order to investigate a large portion of the phase space, we started our LMD simulations from several random Ge-Te atomic configurations by interchanging various atoms and using chemical intuition. In addition, we considered several other, usually high-symmetry, structures from other semiconductor clusters as our starting point for straightforward structural minimization without LMD simulations. In certain cases, the structures obtained from such

studies indeed coincided with results from LMD simulations.

The polarizability calculations for Ge_nTe_m clusters were carried out using a finite-field method.^{19,20} This method is particularly convenient in real-space calculations of confined systems, as the potential due to an external electric field \mathbf{F} can simply be added to the Kohn-Sham Hamiltonian as

$$\left(\frac{-\hbar^2 \nabla^2}{2m} + v_{\text{eff}}(\mathbf{r}) - e\mathbf{F} \cdot \mathbf{r} \right) \phi_n(\mathbf{r}) = \epsilon_n \phi_n(\mathbf{r}), \quad (1)$$

where the effective potential v_{eff} contains the usual ionic, Hartree, and exchange correlation terms, and $\psi_n(\mathbf{r})$ and ϵ_n are the one-electron eigenfunctions and eigenvalues, respectively. The above equation is solved with infinitesimal external electric fields δF_i pointing along all three Cartesian directions, and the total energy E differences obtained allow us to find the dipole moments μ_i and the polarizability tensor α_{ij} from

$$\alpha_{ij} = \frac{\partial \mu_i(F)}{\partial F_j} = -\frac{\partial^2 E(F)}{\partial F_i \partial F_j}, \quad i, j = x, y, z. \quad (2)$$

Since the value measured in experiments is the average polarizability $\langle \alpha \rangle = \frac{1}{3} \text{tr}(\alpha_{ij}) = (\alpha_{xx} + \alpha_{yy} + \alpha_{zz})/3$, it is enough to calculate only the diagonal components α_{ii} of the polarizability tensor. The magnitude of the infinitesimal field δF was chosen as 10^{-3} a.u. For this value of the electric field, the polarizabilities calculated from second-order finite differences of the total energies and first-order differences of the dipole moments fall within 1% of each other.

III. RESULTS AND DISCUSSION

A. Structural properties

The calculated geometries for lowest energy structures of Ge_nTe_m clusters are shown in the Fig. 1. The dimer bond length is calculated to be 2.32 Å (at a grid spacing h of 0.25 a.u.), in agreement with recent calculations of Bálbas, Rubio, and Martins (BRM).¹⁰ The calculated dipole for the dimer, 0.97 debye (D), is also in good agreement with BRM's calculated value of 0.98 D and experimental value of 1.06 ± 0.07 D.²¹ As discussed by BRM, the dipole moment is very sensitive to the bond lengths; e.g., while the calculated bond length at the grid spacing of $h=0.5$ a.u. is less than 1% smaller (2.30 Å), the calculated dipole moment is 0.9 D. Also, the underestimation of the bond length with the LDA is consistent with our calculated dipole moment being slightly smaller than the experimental value. When the calculations are performed with a GGA functional, the dimer bond length increases, as expected, to 2.37 Å, with a corresponding increase in the calculated dipole moment to 1.14 D.

Both clusters with $n+m=3$ atoms, Ge_2Te and GeTe_2 , have a buckled C_{2v} structure, as shown in Fig. 1. The structure and dipole moment for Ge_2Te agree very well with results of BRM: The interatomic distance in the equilateral triangle geometry of this cluster is found to be 2.53 Å in this study, while BRM find a value of 2.52 Å, and the calculated dipole moments are 0.28 D and 0.31 D, respectively. These values are in good agreement with the experimentally mea-

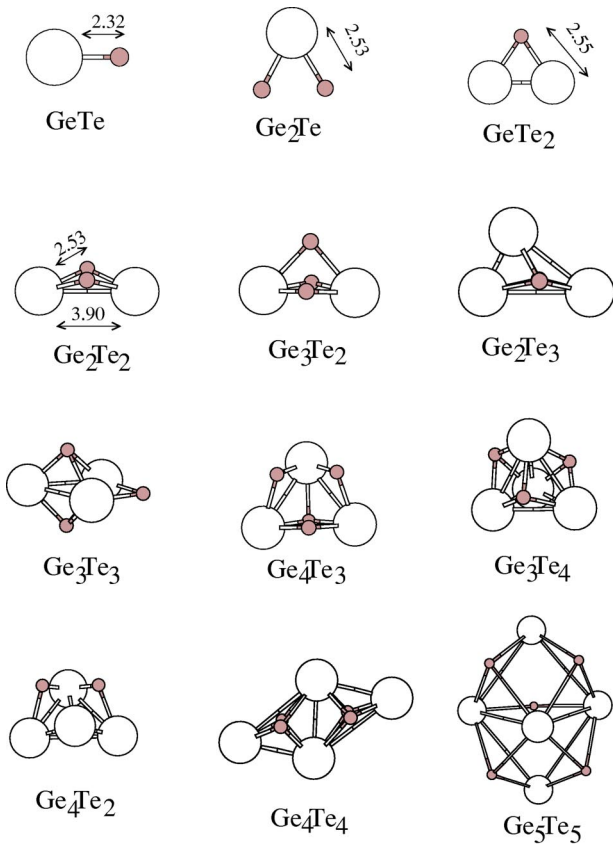


FIG. 1. Calculated ground-state geometries of Ge_nTe_m clusters. The small shaded and large open circles represent Ge and Te atoms, respectively. Distances are given in Å.

sured effective dipole moment of 0.31 ± 0.03 ,³ but not with the permanent dipole moment estimates from a classical analysis. The effect of the GGA is to increase the Ge-Te bond lengths to 2.72 Å, while the Ge-Ge bond length increases to 2.55 Å. For GeTe_2 , on the other hand, our calculated lowest-energy structure of C_{2v} symmetry and a finite dipole moment of 0.99 D is not in agreement with the BRM's result of a linear molecule ($D_{\infty h}$ symmetry) with a vanishing dipole moment. Our calculated lowest-energy C_{2v} structure is lower in energy than a local minimum linear structure by 0.25 eV. In order to eliminate possible sources of discrepancy, we calculated the structural energy differences using the same pseudopotential parameters of BRM. Still, the buckled structure was lower in energy (about 0.3 eV this time) than a linear molecule. The experimental observation that GeTe_2 clusters seem to have no permanent dipole moments suggests that this molecule is probably linear. Therefore, we also examined whether the GGA could change the relative energy ordering of the two structures of GeTe_2 . We found that the GGA actually favors the buckled structure over the linear one more than the LDA, with the calculated GGA energy difference increasing to 0.56 eV. Hence, our finding of the lowest-energy structure with C_{2v} symmetry could be due to experimental conditions (kinetic limitations) somehow sampling the slightly higher-energy linear molecule. Another possibility is that the experiment might be sampling buckled GeTe_2 molecules in which the apex Ge

atoms flip at nonzero temperatures back and forth between two symmetric configurations with opposite dipole moments, resulting in an average zero dipole moment.

For the equilibrium geometry of Ge_2Te_2 we obtained a deformed tetrahedron with C_{2v} geometry as shown in Fig. 1. This structure, for Ge_2Te_2 can be viewed as a distorted (buckled) version of the planar rhombus with D_{2h} symmetry, which has consistently been found as the lowest-energy structure for group IV (such as Si_4 and Ge_4) (Refs. 1,17,19 and 22), group III-IV (Ga_2As_2) (Refs. 19 and 23), and group II-VI (such as Cd_2Se_2 and Cd_2S_2) (Refs. 24 and 25) semiconductor clusters. In this IV-VI semiconductor, the higher-symmetry D_{2h} rhombus is ~ 0.4 eV higher in energy than the buckled C_{2v} structure. The symmetry of our lowest-energy structure as well as the bond lengths agree quite well with the calculations of BRM: Our calculated Ge-Ge, Ge-Te, and Te-Te bond lengths are 3.07 Å, 2.53 Å, and 3.90 Å, while BRM's values are 3.03 Å, 2.57 Å, and 3.87 Å, respectively. Our calculated dipole moment for this geometry is 0.14 D, while BRM find a value of 0.06 D. These values, which as mentioned before are very sensitive to small changes in bond lengths, are in fair agreement with the effective dipole moment of 0.23 D obtained from experiment.

The equilibrium structures for clusters with $n+m \geq 5$ are also shown in Fig. 1. In general, we observe relatively low-symmetry structures, particularly for Te-rich clusters. For example, for five-atom clusters Ge_3Te_2 and Ge_2Te_3 , the symmetries of the lowest-energy structures are found to be C_{2v} and C_{1h} , respectively. Similarly for the seven-atom cluster Ge_4Te_3 the symmetry is only C_{1h} , while Ge_3Te_4 possesses no symmetry at all. The loss of symmetry results in most of these structures having large dipole moments reaching values as large as 1.8 D to 2.0 D for Ge_4Te_3 and Ge_3Te_3 , respectively. The buckled rhombus geometry of Ge_2Te_2 is observed to be a common structural motif in most of these clusters. In general, the structures for Ge_nTe_m clusters assume different and lower-symmetry structures with respect to their group IV, III-V, and II-VI counterparts. Even in cases where the structures look similar (such as Ge_3Te_2 and Ge_4Te_4) the IV-VI cluster always assumes a slightly distorted version of the corresponding group IV or III-V semiconductor. One similarity between these IV-VI and II-VI clusters investigated earlier seems to be the peripheral distribution of the chalcogenide atom Te. We believe this is a direct result of the Coulombic repulsions between the Te atoms, as put forward to explain the similar structural property of Cd_nS_n and Cd_nSe_n clusters.²⁴

B. Electronic properties

The binding energies and HOMO-LUMO energy gaps for Ge_nTe_m clusters are shown in Fig. 2. The binding energies are observed to be generally increasing from ~ 3.3 eV for GeTe to ~ 4.1 eV for Ge_5Te_5 . The local maxima in the binding energies occurring for Ge_3Te_2 , Ge_3Te_3 , and Ge_4Te_3 suggest that these clusters are relatively more stable than clusters of nearby compositions. The relative higher stability of these clusters is also evident when the HOMO-LUMO gaps in the same figure are taken into consideration. It should be

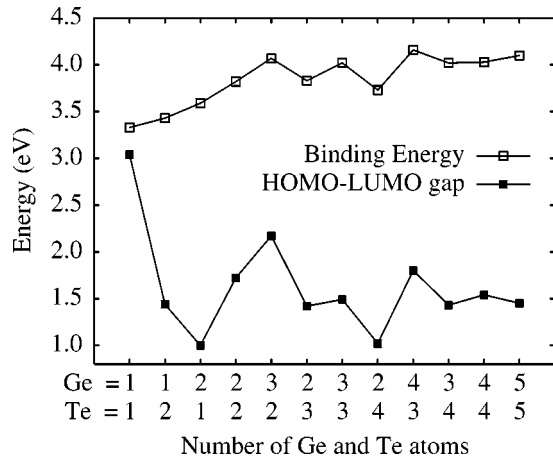


FIG. 2. Binding energies and HOMO-LUMO gaps of Ge_nTe_m clusters.

noted that since the LDA is most likely to underestimate the energy gap, these HOMO-LUMO gap values should not be taken as the gaps to be compared with future experimental work. Generally speaking, structures of higher stability tend to have higher HOMO-LUMO gaps (although this is not a strict rule and can certainly be violated in many systems). An obvious exception to this general observation comes from clusters of two and three atoms. In going from the dimer to the trimer, the HOMO-LUMO gaps drop considerably (by 1.5–2 eV), while the binding energies increase slightly by ~ 0.1 –0.3 eV. Considering clusters with the same total number of atoms, the higher the Ge content, the more stable the structure is, as observed clearly for clusters of five, six, and seven atoms. When the calculations are performed using the GGA functional, we find, as expected, that both the HOMO-LUMO gaps and binding energies drop compared to their LDA values by ~ 0.2 –0.4 eV.

Figure 3 shows the theoretical ($T=0$ K) and experimental³ (at $T_{\text{nozzle}}=300$ and 38 K) polarizabilities α plotted as a function of the cluster size for $n+m \leq 10$ atoms. Compared to group IV, III-V, and II-VI semiconductor clusters, the variation of calculated α in this size regime with cluster size is significantly reduced. For example, the smallest and largest calculated polarizabilities per atom for the clusters considered are 5.37 \AA^3 (Ge_3Te_2) and 6.03 \AA^3 (Ge_4Te_4)—respectively, i.e., a maximum variation of 0.66 \AA^3 . This is in contrast to Si_n , Ge_n ($n \leq 10$), Ga_nAs_m ($n+m \leq 10$; $n=m$, $n=m \pm 1$), and Cd_nSe_m ($n \leq 5$) clusters, where the corresponding variations are 2 \AA^3 , 2 \AA^3 , 1.8 \AA^3 , and 1.6 \AA^3 , respectively.^{19,24,26} Another difference of the calculated polarizabilities for these IV-VI clusters in comparison to other semiconductor clusters is the lack of a monotonic variation of α as a function of the cluster size. In the group IV, III-V, and II-VI semiconductor clusters investigated so far, the calculated polarizabilities decrease quite monotonically as the cluster size increases, approaching the bulk limit from above. This bulk limit α_{bulk} , which is calculated within the dielectric sphere model,³ is 5.85 \AA^3 for GeTe. The calculated α values of Ge_nTe_m clusters, as shown in Fig. 3, are scattered with small fluctuations around α_{bulk} . Examination of Fig. 3 along with the energy gap and binding

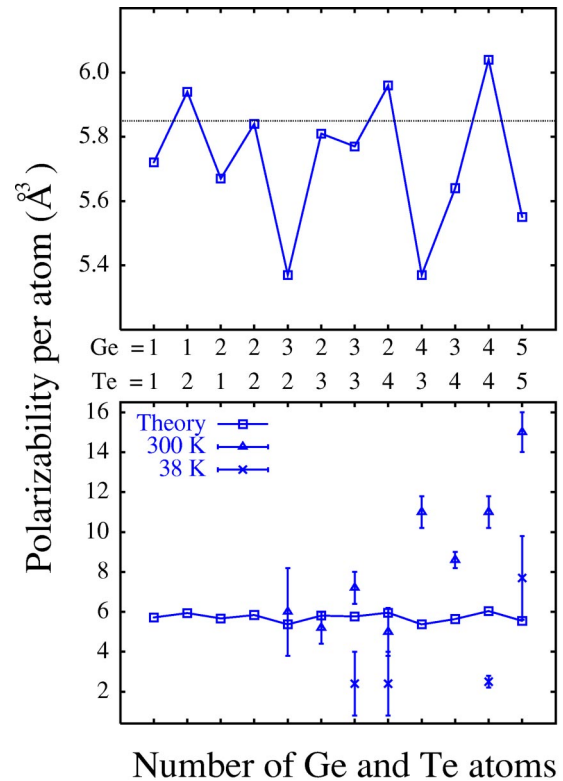


FIG. 3. Polarizabilities α of Ge_nTe_m clusters. The upper panel shows only the theoretical α values scattered with small fluctuations around $\alpha_{\text{bulk}}=5.85 \text{ \AA}^3$, shown by the dotted horizontal line. The lower panel shows (on an extended vertical scale) both theoretical and experimental (Ref. 3) polarizabilities measured at $T_{\text{nozzle}}=38$ and 300 K.

energy data on Fig. 2 shows that the lowest polarizabilities in this size regime are obtained for the two most stable clusters (Ge_3Te_2 and Ge_4Te_3) with the largest HOMO-LUMO energy gaps.

The calculated polarizabilities ($T=0$ K) for a few Ge_nTe_m clusters agree quite well with the experimental polarizabilities within the error bars of the experiment, such as Ge_3Te_2 , Ge_2Te_3 , and Ge_2Te_4 . However, for the rest of the clusters considered, the agreement with experiment is not very good. Interestingly, for Ge_3Te_3 and Ge_2Te_4 , theoretical values have a better agreement with the experimental measurements at $T_{\text{nozzle}}=300$ K than at $T_{\text{nozzle}}=38$ K. In fact, in all the clusters for which the agreement between experiment and theory is not good, the theoretical results are lower than the experimental $T_{\text{nozzle}}=300$ K results, which means that finite-temperature calculations of the polarizability²⁷ and ionic contributions due to large dipole moments^{19,26} can make the agreement between theory and experiment at $T_{\text{nozzle}}=300$ K better. However, polarizabilities measured at $T_{\text{nozzle}}=38$ K, which are $2.4 \pm 1.6 \text{ \AA}^3/\text{atom}$ for Ge_3Te_3 and Ge_2Te_4 , and $2.5 \pm 0.3 \text{ \AA}^3/\text{atom}$ for Ge_4Te_4 are much too small compared to the theoretical values scattered with small fluctuations near α_{bulk} . In addition to the smaller clusters considered here, the measured α at $T_{\text{nozzle}}=38$ K for some of the larger ones, such as Ge_4Te_6 , Ge_5Te_6 , Ge_6Te_6 , Ge_5Te_7 , Ge_7Te_8 , and Ge_7Te_9 , are similarly too small (around 3–

$4 \text{ \AA}^3/\text{atom}$), which poses a very puzzling question as to how such small α values can be obtained for a significant number of Ge_nTe_m clusters. The only exception to this observation is Ge_5Te_5 , for which the theoretical value at 38 K is within the experimental error bars, and the measured α at 300 K seems much too large to be accounted for in terms of dipole moment contributions or temperature effects. Another slightly puzzling issue is the variation of the polarizability for Ge- and Te-rich clusters—namely, the measured α values for Ge-rich clusters are higher than those for Te-rich clusters—whereas the calculations show just the opposite effect (in agreement with the general observation that HOMO-LUMO gaps for Ge-rich clusters are larger than those of Te-rich ones). In short, while the calculations presented here are in agreement with some experimental data and some aspects of the experimental findings (such as calculation of large dipole moments suggesting the experimentally observed strong temperature dependence of α), the actual small magnitudes of low-temperature polarizabilities and some anomalously large high-temperature polarizabilities still remain a mystery.

As stated in the previous section, the calculated ground-state structures of Ge_nTe_m clusters have lower symmetries compared to other semiconductor clusters. At a given composition, the potential energy surfaces of Ge_nTe_m clusters possess local minima corresponding to higher-symmetry structures. The symmetry breaking for the global minimum is accompanied by a considerable gain in electronic energy and (usually) a widening of the HOMO-LUMO gap, reminiscent of the Peierls distortion observed in solid and liquid GeTe. This general observation is illustrated by considering the particular clusters GeTe_2 , Ge_2Te , Ge_2Te_2 , and Ge_2Te_3 in Fig. 4. For the case of trimers GeTe_2 and Ge_2Te , the structures with buckled C_{2v} symmetry are lower in energy than the linear structures of $D_{\infty h}$ symmetry by 0.25 eV and 2.15 eV, respectively. For the tetramer Ge_2Te_2 , the structure of lower C_{2v} symmetry is energetically more favorable than a planar structure of D_{2h} symmetry by 0.4 eV. Similarly, for the pentamer Ge_2Te_3 , the C_{1h} symmetry structure has a lower energy than a structure of D_{3h} symmetry by 0.45 eV. Except for GeTe_2 , the lower-energy structures in Fig. 4 also have larger HOMO-LUMO gaps compared to more symmetric higher-energy structures. For example, the linear Ge_2Te has an almost vanishing gap, while the buckled Ge_2Te has a gap of 1 eV. In Ge_2Te_2 and Ge_2Te_3 , the increase in the gaps in going from the high- to low-symmetry structures are 0.75 eV and 1.3 eV, respectively. The only exception to this general observation comes from the linear versus buckled structures of GeTe_2 . While we consistently (with respect to the LDA versus the GGA, different pseudopotential, reduced h , etc.) find the buckled GeTe_2 lower in energy than the linear one, the linear GeTe_2 has a surprisingly large HOMO-LUMO gap of 2.5 eV, which is larger than that of the buckled structure by ~ 1.1 eV.

The relative stability of lower-symmetry structures in Ge_nTe_m clusters can also be expected to manifest itself in the vibrational frequencies of particular modes for the high- and low-symmetry structures. In fact, one of the possible explanations for the strong temperature dependence of polarizabilities of certain Ge_nTe_m clusters^{3,28} is based on some kind of an ionic instability in analogy with the transverse optical

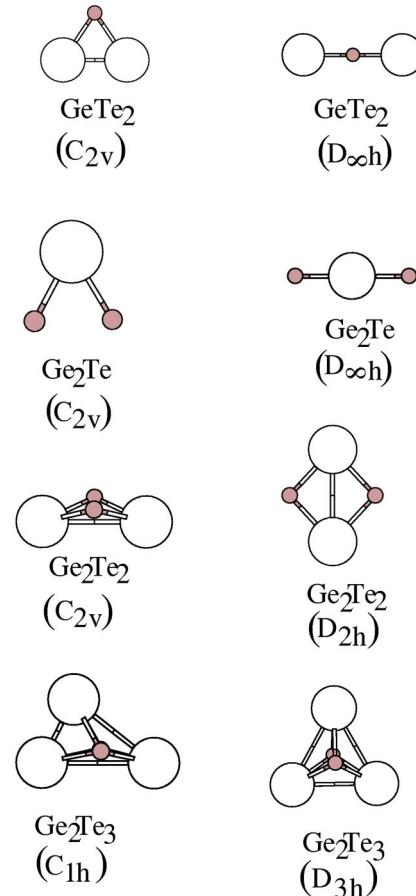


FIG. 4. Geometries and symmetries of ground state structures (left column) in comparison to some higher-energy isomers (right column) of GeTe_2 , Ge_2Te , Ge_2Te_2 , and Ge_2Te_3 clusters.

phonon softening observed in the bulk $B1$ to $A7$ phase transition.⁵ A complete determination of the vibrational frequencies for all ground-state and local minima clusters is a major task; hence, we considered only one prototype example (from Fig. 4) to calculate its vibrational frequencies in the high- and low-symmetry structures: namely, Ge_2Te_2 in the planar (D_{2h}) and buckled (C_{2v}) geometries. In order to obtain the vibrational frequencies, we calculated the dynamical matrix $D_{i\alpha,j\beta}$ given by the second-order derivative of the total energy E or the first-order derivative of the forces with respect to ionic displacements as

$$D_{i\alpha,j\beta} = \frac{1}{m_i} \frac{\partial^2 E}{\partial R_i^\alpha \partial R_j^\beta} = - \frac{1}{m_i} \frac{\partial F_i^\alpha}{\partial R_j^\beta}, \quad (3)$$

where R_i^α and F_i^α represent the displacement of and the force on atom i in the α direction. Diagonalization of $D_{i\alpha,j\beta}$ gives the vibrational frequencies and the corresponding eigenmodes.²⁹

The results for the six vibrational frequencies of Ge_2Te_2 in the two structures are summarized in Table I, and Fig. 5 shows the relevant eigenmodes for the D_{2h} planar structure. In general, the modes become softer in going from the C_{2v} structure to the D_{2h} structure, but major softenings are observed in the two modes A_g and B_{3u} of the D_{2h} structure, which are at 92 cm^{-1} and 80 cm^{-1} , respectively. The corre-

TABLE I. Vibrational frequencies (in cm^{-1}) and corresponding normal modes for the planar D_{2h} and buckled C_{2v} structures of Ge_2Te_2 .

Mode	D_{2h}		C_{2v}	
	Frequency	Mode	Frequency	Mode
B_{3u}	80	B_1	175	
A_g	92	A_1	198	
B_{3g}	192	B_2	204	
A_g	234	A_1	275	
B_{2u}	242	B_2	224	
B_{1u}	246	A_1	288	

sponding modes in the C_{2v} structure (A_1 and B_1 from the compatibility relations) are more than twice these values, at 175 cm^{-1} and 192 cm^{-1} , respectively. Not surprisingly, these modes correspond to into- and out-of-plane (B_{3u}) and in-plane out-of-phase pairing (A_g) motions of the Ge and Te atoms. While the vibrational frequency for the B_{3u} mode is still real—hence the planar D_{2h} structure is stable with respect to Ge and Te atoms moving along the $\pm z$ -directions—the mode is very soft compared to the corresponding B_1 mode in the buckled structure. This indicates the tendency of the planar D_{2h} structure to distort to a lower-symmetry structure, in which the distortions of Ge and Te atoms, as suggested by the B_{3u} eigenmodes, are indeed as those observed in the buckled C_{2v} structure. This is an interesting manifestation of Peierls distortion observed in both solid and liquid phases of GeTe in its metastable cluster phase. In addition, in going from the D_{2h} to the C_{2v} structures, the Ge-Ge interatomic distance decreases by $\sim 0.4 \text{ \AA}$, while the Te-Te distance increases slightly. These relaxations do indeed correspond to the other soft mode (A_g) of the D_{2h} structure at 92 cm^{-1} . These observations suggest that further examinations of the vibrational frequencies and modes in low- and high-symmetry structures will be very instructional and could be useful in understanding the strong temperature dependence of polarizabilities for particular sizes of Ge_nTe_m clusters.

IV. SUMMARY

In summary, we have performed a detailed investigation of structural and electronic properties of small Ge_nTe_m ($n + m \leq 10$) clusters in real space using an *ab initio* pseudopotential total energy method and Langevin molecular dynamics coupled to a simulated annealing procedure. Various properties of these group IV-VI clusters, such as geometries

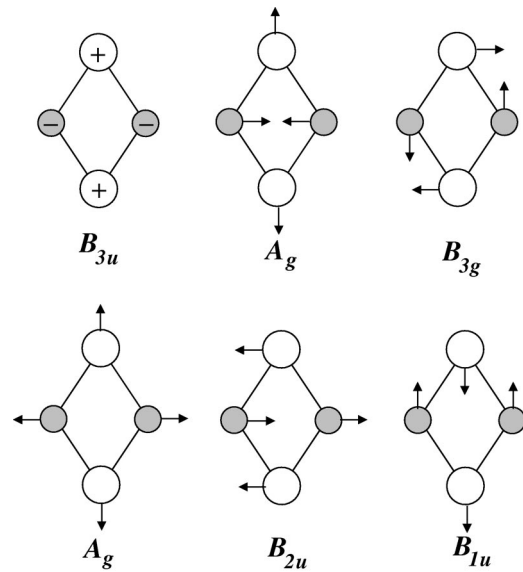


FIG. 5. The vibrational modes of Ge_2Te_2 in its planar structure of D_{2h} symmetry. The smaller shaded and larger open circles represent Ge and Te, respectively. The + and - signs for the B_{3u} mode represent the perpendicular motions of Te and Ge atoms in and out of the plane.

of ground-state and low-energy isomer structures, dipole moments, binding energies, HOMO-LUMO gaps, static polarizabilities, and vibrational frequencies, were calculated. While the calculated polarizabilities agree well for some of the clusters with experimental data, most of the experimental values at $T_{\text{nozzle}} = 38 \text{ K}$ remain much too small compared to the theoretical values. Furthermore, while some of the large polarizabilities measured at 300 K can be explained through ionic contributions due to large dipole moments and temperature effects, some polarizabilities remain anomalously large with respect to theoretical values. Our calculations show that Ge_nTe_m clusters tend to adopt low-symmetry structures with large dipole moments when compared with group IV, III-V, and II-VI semiconductor clusters. Examination of binding energies, HOMO-LUMO gaps, and vibrational frequencies for ground-state and higher-symmetry structures of selected clusters indicates that this tendency can be attributed to Peierls distortions, which are also observed in the solid and liquid phases of GeTe. This fascinating behavior of Ge_nTe_m clusters for larger sizes as well as the unresolved discrepancies regarding the polarizabilities measured at $T_{\text{nozzle}} = 38$ and 300 K suggests that further theoretical and experimental studies are necessary to achieve a better understanding of the rich physics and chemistry of these IV-VI semiconductor clusters.

¹M. Jarrold, *Science* **252**, 1085 (1991).

²B. Hartke, *Angew. Chem., Int. Ed. Engl.* **41**, 1468 (2002).

³R. Schäfer, S. Schlecht, J. Woenckhaus, and J.A. Becker, *Phys. Rev. Lett.* **76**, 471 (1996).

⁴M. Broyer, R. Antoine, E. Benichou, I. Compagnon, P. Dugourd,

and D. Rayane, *C. R. Phys. (Paris)* **3**, 301 (2002).

⁵P.B. Littlewood and V. Heine, *J. Phys. C* **12**, 4431 (1979).

⁶R. E. Peierls, *Quantum Theory of Solids* (Clarendon, Oxford, 1955), p. 108.

⁷J.-P. Gaspard, A. Pellegratti, F. Marinelli, and C. Bichara, *Philos.*

- Mag. B **77**, 727 (1988).
- ⁸J.Y. Raty, V. Godlevsky, P. Ghosez, C. Bichara, J.P. Gaspard, and J.R. Chelikowsky, Phys. Rev. Lett. **85**, 1950 (2000).
- ⁹J.Y. Raty, V.V. Godlevsky, J.P. Gaspard, C. Bichara, M. Bionducci, R. Bellissent, R. Céolin, J.R. Chelikowsky, and Ph. Ghosez, Phys. Rev. B **65**, 115205 (2002).
- ¹⁰L.C. Bálbas, A. Rubio, and J.L. Martins, Z. Phys. D: At., Mol. Clusters **40**, 182 (1997).
- ¹¹J.R. Chelikowsky, N. Troullier, and Y. Saad, Phys. Rev. Lett. **72**, 1240 (1994); J.R. Chelikowsky, N. Troullier, K. Wu, and Y. Saad, Phys. Rev. B **50**, 11 355 (1994).
- ¹²N. Troullier and J.L. Martins, Phys. Rev. B **43**, 1993 (1991).
- ¹³L. Kleinman and D.M. Bylander, Phys. Rev. Lett. **48**, 1425 (1982).
- ¹⁴S.G. Louie, S. Froyen, and M.L. Cohen, Phys. Rev. B **26**, 1738 (1982).
- ¹⁵D.M. Ceperley and B.J. Alder, Phys. Rev. Lett. **45**, 566 (1980).
- ¹⁶J.P. Perdew, K. Burke, and M. Ernzerhof, Phys. Rev. Lett. **77**, 3865 (1996).
- ¹⁷N. Binggeli, J.L. Martins, and J.R. Chelikowsky, Phys. Rev. Lett. **68**, 2956 (1992).
- ¹⁸D.F. Shanno and K.-H. Phua, Math. Program. **14**, 149 (1978).
- ¹⁹I. Vasiliev, S. Ögüt, and J.R. Chelikowsky, Phys. Rev. Lett. **78**, 4805 (1997).
- ²⁰H.A. Kurtz, J.J.P. Stewart, and K.M. Dieter, J. Comput. Chem. **96**, 231 (1990); A.A. Quong and M.R. Pederson, Phys. Rev. B **46**, 12 906 (1992); I. Moullet, J.L. Martins, F. Reuse, and J. Buttet, *ibid.* **42**, 11 598 (1990); D. Porezag and M.R. Pederson, *ibid.* **54**, 7830 (1996).
- ²¹J. Hoefl, F.J. Lovas, E. Tiemann, and T. Törring, Z. Naturforsch. A **25**, 539 (1970).
- ²²P.W. Deutsch, L.A. Curtiss, and J.P. Blaudeau, Chem. Phys. Lett. **344**, 101 (2001); B.X. Li and P.L. Cao, Phys. Rev. B **62**, 15 788 (2000); S. Ögüt and J.R. Chelikowsky, *ibid.* **55**, R4914 (1997); P. Ballone, W. Andreoni, R. Car, and M. Parrinello, Phys. Rev. Lett. **60**, 271 (1988); R. Fournier, S.B. Sinnott, and A.E. DePristo, J. Chem. Phys. **97**, 4149 (1992); G. Pacchioni and J. Koutecky, *ibid.* **84**, 3301 (1986); K. Raghavachari, *ibid.* **84**, 5672 (1986).
- ²³J.Y. Yi, Chem. Phys. Lett. **325**, 269 (2000); P. Piquini, S. Canuto, and A. Fazzio, Nanostruct. Mater. **10**, 635 (1998); K.M. Song, A.K. Ray, and P.K. Khowash, J. Phys. B **27**, 1637 (1994); W. Andreoni, Phys. Rev. B **45**, 4203 (1992); L. Lou, L. Wang, L.P.F. Chibante, R.T. Laaksonen, P. Nordlander, and R.E. Smalley, J. Chem. Phys. **94**, 8015 (1991); **95**, 6602 (1991).
- ²⁴M.C. Tropicovsky and J.R. Chelikowsky, J. Chem. Phys. **114**, 943 (2001).
- ²⁵P. Deglmann, R. Ahlrichs, and K. Tsereteli, J. Chem. Phys. **116**, 1585 (2002); J.M. Matxain, J.E. Fowler, and J.M. Ugalde, Phys. Rev. A **61**, 053201 (2000); V.S. Gurin, Int. J. Quantum Chem. **71**, 37 (1999).
- ²⁶A. Sieck, D. Porezag, Th. Frauenheim, M.R. Pederson, and K. Jackson, Phys. Rev. A **56**, 4890 (1997); K. Jackson, M. Pederson, C.Z. Wang, and K.M. Ho, *ibid.* **59**, 3685 (1999).
- ²⁷L. Kronik, I. Vasiliev, and J.R. Chelikowsky, Phys. Rev. B **62**, 9992 (2000).
- ²⁸J.A. Becker, S. Schlecht, R. Schäfer, J. Woenckhaus, and F. Hensel, Mater. Sci. Eng., A **127/128**, 1 (1996).
- ²⁹X. Jing, N. Troullier, J.R. Chelikowsky, K. Wu, and Y. Saad, Solid State Commun. **96**, 231 (1995); J.R. Chelikowsky, X. Jing, K. Wu, and Y. Saad, Phys. Rev. B **53**, 12 071 (1996).